university of groningen

University Medical Center Groningen

University of Groningen

# Catalytic Depolymerization of Lignin and Woody Biomass in Supercritical Ethanol

Huang, Xiaoming; Atay, Ceylanpinar; Zhu, Jiadong; Palstra, Sanne W L; Korányi, Tamás I; Boot, Michael D; Hensen, Emiel J M

*Published in:*
ACS Sustainable Chemistry & Engineering

*DOI:*
10.1021/acssuschemeng.7b02790

**IMPORTANT NOTE: You are advised to consult the publisher's version (publisher's PDF) if you wish to cite from it. Please check the document version below.**

*Document Version*
Publisher's PDF, also known as Version of record

*Publication date:*
2017

Link to publication in University of Groningen/UMCG research database

*Citation for published version (APA):*
Huang, X., Atay, C., Zhu, J., Palstra, S. W. L., Korányi, T. I., Boot, M. D., & Hensen, E. J. M. (2017). Catalytic Depolymerization of Lignin and Woody Biomass in Supercritical Ethanol: Influence of Reaction Temperature and Feedstock. *ACS Sustainable Chemistry & Engineering* , *5*(11), 10864-10874. https://doi.org/10.1021/acssuschemeng.7b02790

**Copyright**
Other than for strictly personal use, it is not permitted to download or to forward/distribute the text or part of it without the consent of the author(s) and/or copyright holder(s), unless the work is under an open content license (like Creative Commons).

The publication may also be distributed here under the terms of Article 25fa of the Dutch Copyright Act, indicated by the “Taverne” license. More information can be found on the University of Groningen website: https://www.rug.nl/library/open-access/self-archiving-pure/taverne-amendment.

**Take-down policy**
If you believe that this document breaches copyright please contact us providing details, and we will remove access to the work immediately and investigate your claim.

*Downloaded from the University of Groningen/UMCG research database (Pure): http://www.rug.nl/research/portal. For technical reasons the number of authors shown on this cover page is limited to 10 maximum.*

Download date: 12-10-2022

This is an open access article published under a Creative Commons Non-Commercial No Derivative Works (CC-BY-NC-ND) Attribution License, which permits copying and redistribution of the article, and creation of adaptations, all for non-commercial purposes.

ACS Sustainable Chemistry & Engineering

Research Article

Cite This: ACS Sustainable Chem. Eng. 2017, 5, 10864-10874

pubs.acs.org/journal/ascecg

# Catalytic Depolymerization of Lignin and Woody Biomass in Supercritical Ethanol: Influence of Reaction Temperature and Feedstock

Xiaoming Huang,[†] Ceylanpinar Atay,[‡] Jiadong Zhu,[†] Sanne W. L. Palstra,[§] Tamás I. Korányi,[†] Michael D. Boot,[∥] and Emiel J. M. Hensen*[,†]

[†]Schuit Institute of Catalysis, Inorganic Materials Chemistry, Eindhoven University of Technology, P. O. Box 513, 5600 MB Eindhoven, The Netherlands

[‡]Chemical Engineering Department, Istanbul Technical University, Maslak, 34469, Istanbul, Turkey

[§]Centre for Isotope Research, Energy and Sustainability Research Institute Groningen, University of Groningen, Nijenborgh 6, 9747 AG Groningen, The Netherlands

[∥]Combustion Technology, Department of Mechanical Engineering, Eindhoven University of Technology, P.O. Box 513, 5600 MB Eindhoven, The Netherlands

**ABSTRACT:** The one-step ethanolysis approach to upgrade lignin to monomeric aromatics using a CuMgAl mixed oxide catalyst is studied in detail. The influence of reaction temperature (200−420 °C) on the product distribution is investigated. At low temperature (200−250 °C), recondensation is dominant, while char-forming reactions become significant at high reaction temperature (>380 °C). At preferred intermediate temperatures (300−340 °C), char-forming reactions are effectively suppressed by alkylation and Guerbet and esterification reactions. This shifts the reaction toward depolymerization, explaining high monomeric aromatics yield. Carbon-14 dating analysis of the lignin residue revealed that a substantial amount of the carbon in the lignin residue originates from reactions of lignin with ethanol. Recycling tests show that the activity of the regenerated catalyst was strongly decreased due to a loss of basic sites due to hydrolysis of the MgO function and a loss of surface area due to spinel oxide formation of the Cu and Al components. The utility of this one-step approach for upgrading woody biomass was also demonstrated. An important observation is that conversion of the native lignin contained in the lignocellulosic matrix is much easier than the conversion of technical lignin.

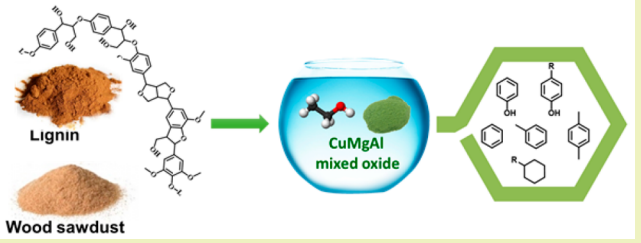


**KEYWORDS:** *Biomass, Lignin, Supercritical ethanol, Alkylation, Guerbet reaction*

## INTRODUCTION

Lignin is a complex amorphous three-dimensional network polymer, which is mainly composed of phenylpropane units, which are nonlinearly and randomly linked to each other by C−C and C−O−C bonds.[1] In plants, lignin serves as the glue in the lignocellulosic matrix providing structural integrity, waterproofing properties, and resilience to environmental attack. Industrial (technical) lignin is mainly obtained as the byproduct in the paper and pulping industry.[2] The amount of available lignin will rapidly increase when more second-generation bioethanol processes come on stream.[3] Lignin already finds application as biobased starting material for the manufacture of dispersants, wood panels, emulsifiers, polyurethane foams, automotive brakes, and epoxy resins.[4,5] Apart from these, another promising approach is to depolymerize lignin into aromatic compounds such as benzene, toluene, xylenes, and phenols, which may serve as fuels and base chemicals.

In the past 2 decades, numerous approaches have been put forward to add value to lignin by chemical conversion into smaller molecules.[3,4,6−10] The main conversion routes include gasification, pyrolysis, and acid- or base-catalyzed oxidative or reductive depolymerization. Among these, reductive depolymerization has been most frequently explored in recent years. Solvents such as sub- and supercritical water,[11−14] methanol,[15−18] ethanol,[17,19−22] 2-propanol,[17,23] ethanol/water,[24−27] dioxane,[28,29] methanol/water,[30] formic acid/ethanol,[2,31] and water/dioxane[32] were investigated as medium for lignin solvolysis and hydrogenolysis. Both precious group metals (Pd, Pt, Ru, and Rh, etc.) and more abundant metals (Cu, Ni, and Mo, etc.) can catalyze the involved hydrogenolysis reactions. Raney Ni,[23,33,34] Ni−*Me* (*Me* = Ru, Rh, and Pd),[14,35] Ni/C,[17] $\alpha$-$MoC_{1-x}$,[20,36] $Ni/SiO_2-ZrO_2$,[37] Ni/HTC,[38] Cu/Mo-ZSM-5,[39] TiN−Ni[40] and NiMo,[31,41] and CoMo[41] were identified as promising catalysts. Also combinations of supported metal catalysts with homogeneous catalysts such as $Pt/Al_2O_3-H_2SO_4$,[24] Ru/C−NaOH,[42] Ni/ZSM-5−

Received: August 14, 2017
Revised: September 27, 2017
Published: October 9, 2017


© 2017 American Chemical Society

DOI: 10.1021/acssuschemeng.7b02790
ACS Sustainable Chem. Eng. 2017, 5, 10864−10874

**Table 1. Yield of Monomers, Lignin Residues, and Char and the Total Yield Following Lignin Depolymerization as a Function of Temperature with and without Catalyst**

| | | | | | yield of products (wt%) | | | | |
|---|---|---|---|---|---|---|---|---|---|
| entry | catalyst | temp (°C) | $P_{hot}$ (bar) | time (h) | monomers | THF-soluble residue | THF-insoluble residue | char | total yield (wt %) |
| | | | | Reactions in 50 mL Autoclave[a] | | | | | |
| 1 | blank | 200 | 42 | 4 | 2 | 49 | 0 | 26 | 77 |
| 2 | blank | 250 | 70 | 4 | 4 | 39 | 0 | 35 | 78 |
| 3 | blank | 300 | 98 | 4 | 6 | 30 | 0 | 41 | 78 |
| 4 | blank | 340 | 115 | 4 | 8 | 15 | 0 | 36 | 58 |
| 5 | $Cu_{20}MgAl(2)$ | 200 | 44 | 4 | 1 | 21 | 41 | 1 | 64 |
| 6 | $Cu_{20}MgAl(2)$ | 250 | 82 | 4 | 3 | 35 | 59 | 1 | 98 |
| 7 | $Cu_{20}MgAl(2)$ | 300 | 104 | 4 | 17 | 73 | 18 | 0 | 108 |
| 8 | $Cu_{20}MgAl(2)$ | 340 | 140 | 4 | 20 | 69 | 9 | 3 | 101 |
| | | | | Reactions in 100 mL Autoclave[b] | | | | | |
| 9 | $Cu_{20}MgAl(2)$ | 300 | 127 | 4 | 19 | 67 | 11 | 0 | 97 |
| 10 | $Cu_{20}MgAl(2)$ | 340 | 168 | 4 | 30 | 72 | 8 | 1 | 111 |
| 11 | $Cu_{20}MgAl(2)$ | 380 | 234 | 4 | 42 | 56 | 1 | 6 | 105 |
| 12 | $Cu_{20}MgAl(2)$ | 420 | 307 | 4 | 49 | 55 | 0 | 12 | 116 |
| 13 | $Cu_{20}MgAl(2)$ | 380 | 241 | 8 | 60 | 52 | 1 | 10 | 123 |
| 14 | $Cu_{20}MgAl(2)$ | 380 | 258 | 20 | 49 | 47 | 1 | 18 | 115 |
| 15 | $Cu_{20}MgAl(2)$[c] | 380 | 200 | 8 | 39 | 43 | 0 | 10 | 92 |
| 16 | $Cu_{20}MgAl(2)$[d] | 380 | 171 | 8 | 16 | 33 | | | |

[a]50 mL autoclave conditions: 1 g of lignin, 0.5 g of catalyst, and 20 mL of solvent. [b]100 mL autoclave conditions: 1 g of lignin, 0.5 g of catalyst, and 40 mL of solvent. [c]Regenerated catalyst from entry 13. [d]Regenerated catalyst from entry 15.

NaOH,[43] and Pd/C−$ZnCl_2$,[44] and Pd/C−$H_3PO_4$[45] can be used. Most of these approaches target the catalytic conversion of isolated lignin into smaller, usually aromatic, molecules. To achieve reasonable yield, relatively harsh conditions are usually required when technical lignin is the starting material.

Another interesting strategy is to start from raw lignocellulosic biomass and first extract lignin fragments from the native lignin part followed by depolymerization of these simpler molecules into aromatics.[44−50] In this field, the one-pot lignin-first approach, which combines solvolytic extraction and reductive depolymerization of lignin in the presence of hydrogen and a supported metal catalyst, has recently attracted substantial attention. A substantial part of lignin can be extracted from biomass and converted into monoaromatics (e.g., yields ∼ 50% monomer based on lignin content for hardwoods), leaving behind a cellulose-rich pulp. Other researchers reported about one-step conversion of the whole biomass in alcoholic solvents under harsh conditions yielding a more complex mixture of aromatics, alkanes, and alcohols.[16,51,52]

Earlier, we demonstrated a technology that is able to obtain predominantly monoaromatics from isolated lignin using a CuMgAl mixed oxide catalyst in supercritical ethanol.[19,53,54] This approach was inspired by the methanol-mediated conversion of lignin using a similar mixed oxide catalyst by the Ford group.[16] The replacement of methanol by ethanol is beneficial, because ethanol acts as a capping agent and formaldehyde scavenger, thereby suppressing char formation.[54] Several important aspects of this approach such as the influence of reaction temperature, the fate of the ethanol solvent, and possible deactivation of the catalyst have not been discussed yet. As a continuation study of our previous work, we report herein a more detailed analysis of lignin ethanolysis. An important aspect of lignin conversion is the recalcitrant nature of technical lignin which requires harsh conditions to cleave the predominant C−C bonds. At high temperature, solvent conversion can become problematic. In our earlier work, we demonstrated self-condensation of ethanol and alkylation of aromatics. In order to determine how much ethanol is included in lignin-derived products, we employ here for the first time in the context of lignin upgrading the carbon-14 dating technique. We focus on providing more insight into the above-mentioned aspects of lignin ethanolysis but also discuss preliminary results of woody biomass conversion in supercritical ethanol.

## RESULTS AND DISCUSSIONS

**Influence of Reaction Temperature.** Table 1 summarizes the catalytic results for soda lignin conversion in supercritical ethanol. A workup procedure was developed to distinguish smaller, tetrahydrofuran (THF)-soluble and larger (THF-insoluble) lignin fragments and char.[54] The THF-soluble residue contains lignin fragments with a lower molecular weight than the original lignin. The THF-insoluble residue is a fraction that is strongly adsorbed on the solid catalyst and, therefore, cannot be dissolved in THF. After digesting the solid catalyst in nitric acid, this solid fraction becomes THF-soluble. It has a higher molecular weight than the starting lignin as it originates from condensation of lignin fragments. Char is characterized by the fraction that is strongly adsorbed to the solid catalyst and cannot be washed away by THF after digestion of the catalyst in nitric acid. The char nature is emphasized by the lowest H/C ratio among the different solid fractions. The amount of char was determined by thermogravimetric analysis (TGA).[54]

We optimized the reaction temperature of the ethanol solvolysis reaction toward high yield of monoaromatics. To this end, we first investigated the influence of the reaction temperature using a 50 mL high-pressure autoclave. The temperature was varied from 200 to 340 °C, the latter temperature being the maximum temperature of the used autoclave. Without catalyst, an increase of the reaction temperature led to higher lignin monomers yields but also more char, while the amount of THF-soluble lignin residue decreased (Table 1, entries 1−4). This result illustrates that


DOI: 10.1021/acssuschemeng.7b02790
ACS Sustainable Chem. Eng. 2017, 5, 10864−10874

both lignin depolymerization and repolymerization rates are enhanced at higher temperature. Char-forming reactions dominate in the absence of a catalyst. Since char sticks to the internal reactor parts, it cannot be quantitatively recovered from the experiment, explaining the low mass balance. In the presence of the $Cu_{20}MgAl(2)$ catalyst, the monomers yield increases with reaction temperature (Table 1, entries 5−8). Because we expected that even higher monomers yield could be achieved at higher temperature, we employed a high-temperature autoclave. The performance obtained at 300 and 340 °C (Table 1, entries 9 and 10) in this slightly larger autoclave was better than the corresponding experiments in the smaller autoclave (Table 1, entries 7 and 8), likely because of the higher solvent to lignin ratio, which results in better solubility of the lignin, and a higher operating pressure (Table 1). The hot pressure reached in the larger autoclave was significantly higher than in the smaller one, which is the consequence of the higher amount of ethanol and the more extensive re-forming into hydrogen-rich gaseous products during the reaction. The latter is confirmed by analyzing the gas cap of the autoclave after the reaction. Higher hydrogen pressure facilitates hydrogenolysis reactions, which effectively improves lignin monomers yield. At higher temperatures, the lignin monomers yield further improved due to more efficient thermocatalytic/thermal cracking of the most recalcitrant fraction of lignin. A monomer yield of 42 wt % was obtained when increasing the reaction temperature to 380 °C. Further increasing the temperature to 420 °C resulted in a monomers yield of 49 wt %. Figure 1

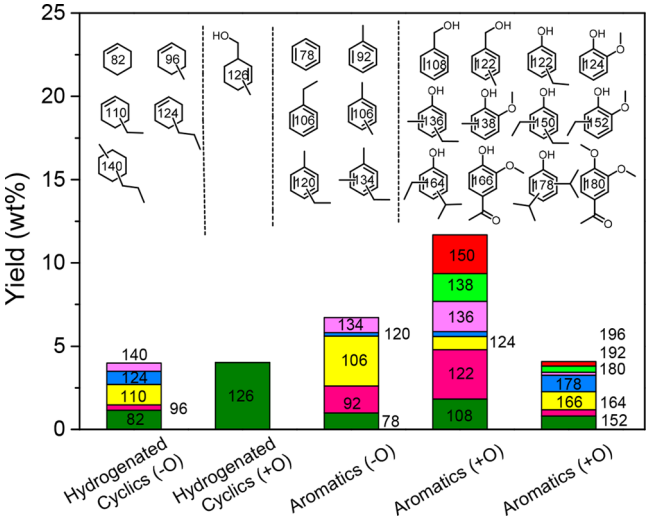


**Figure 1.** Lignin monomers distribution deriving from conversion of P1000 lignin at 340 °C for 4 h over the $Cu_{20}MgAl(2)$ catalyst (Table 1, entry 10).

shows a typical lignin-derived product distribution of the monomer fraction of the products obtained after reaction at 340 °C for 4 h over $Cu_{20}MgAl(2)$. The main products were aromatics with hydrogenated cyclic products as the main side products. Most of these products were alkylated with methyl and/or ethyl groups substituted on the rings.

The THF-insoluble lignin residue was the dominant solid fraction after low-temperature reaction (200−250 °C). This fraction became less dominant at moderate temperature (300−340 °C) while it did not lead to char formation. At higher temperature (380−420 °C), almost no THF-insoluble lignin residue was recovered and, instead, significant amounts of char (6−10 wt %) formed. These changes in the product distribution are very similar to those observed for lignin pyrolysis.[55] In this area, it is known that condensation, depolymerization, and carbonization (formation of compounds with multiple aromatic rings) start at 250, 350, and 400 °C, respectively.[55] A mechanistic study using model lignin compounds revealed that condensation reactions at lower temperature relate to the reactivity of conjugated $C_{\alpha}{=}C_{\beta}$ and phenolic OH groups. Char formation at high temperature is due to carbonization reactions leading to polyaromatics.[55]

We characterized the different types of lignin residue in more detail by GPC. The results are summarized in Table 2. For

**Table 2. GPC Analysis of the Lignin Residues Obtained from Reactions at Different Temperatures for 4 h over the CuMgAl Mixed Oxide Catalyst**

| | | | THF-soluble residue | | THF-insoluble residue | |
|---|---|---|---|---|---|---|
| entry | temp (°C) | reactor vol (mL) | yield (wt %) | $M_w$ (g/mol) | yield (wt %) | $M_w$ (g/mol) |
| 1 | 200 | 50 | 21 | 3376 | 41 | 4071 |
| 2 | 250 | 50 | 35 | 1475 | 59 | 13325 |
| 3 | 300 | 50 | 73 | 1269 | 18 | 21142 |
| 4 | 340 | 50 | 69 | 926 | 9 | 32514 |
| 5 | 380 | 100 | 56 | 475 | 1 | - |
| 6 | 420 | 100 | 55 | 486 | 0 | - |

comparison, the starting P1000 lignin material was also analyzed by using the THF as solvent. As soda lignin is partially soluble in THF, only the THF-soluble fraction was analyzed. The $M_w$ of this fraction is 1100 g/mol. After derivatization by acetylation, lignin became fully soluble in THF with a $M_w$ of 6310 g/mol, in good agreement with the result of the same lignin reported in another recent study.[56] It should be noted that the acetylation step will increase the molecular weight to some extent, depending on the number of OH groups in the lignin. Alkaline size exclusion chromatography (SEC) analysis by using 0.5 M NaOH as solvent has been proposed to be a more accurate method to determine the molecular weight of lignin, as it does not require derivatization.[56] The determined $M_w$ of the same (nonacetyated) soda lignin was 3270 g/mol.[56] For the lignin residue recovered from THF, the THF-based GPC method is preferred, because it gives results similar to those of the alkaline SEC method.[56] The GPC analysis of the THF-soluble lignin residue shows that the $M_w$ decreased with increasing reaction temperature (Table 2). This is in line with the improved monomers yield due to increased depolymerization degree at high reaction temperature. On the other hand, the $M_w$ of the THF-insoluble lignin residue increased at higher temperature (Table 2), which ultimately resulted in char formation in the 380−420 °C range.

Based on the changes in the yield of THF-insoluble residue and char, we conclude that condensation reactions dominate at low reaction temperature (200−250 °C), while char-forming carbonization reactions become significant at high reaction temperature (380−420 °C). At low temperature, lignin depolymerization mainly comprises catalytic hydrogenolysis reactions. The rate of thermolysis is much lower compared with the rate of condensation reactions involving reactive side chains such as C=C double bonds[55] and other reactive species such as formaldehyde.[54] These condensation reactions are favored at low temperature. Another aspect is that reactions that hinder


DOI: 10.1021/acssuschemeng.7b02790
ACS Sustainable Chem. Eng. 2017, 5, 10864−10874

repolymerization such as alkylation, Guerbet, esterification reactions occur also at too low rates when the temperature is low. The lower activity in depolymerization and char-hindering reactions leads to a large contribution of products due to condensation. At moderate reaction temperature (300−340 °C), depolymerization reactions are enhanced and more recalcitrant lignin structures can be cleaved, generating more lignin fragments and reactive phenolic intermediates. These reactive phenolic intermediates can be protected by the enhanced alkylation and Guerbet and esterification reactions. This shifts the reaction balance toward depolymerization, which explains the decreased yield of THF-insoluble residue and increased yields of THF-soluble residue and monomers. The increased rate of protection of lignin monomers was further confirmed by analyzing the lignin residue using radiocarbon dating , to be discussed below. At high temperature (380−420 °C), char-forming reactions become dominant. It is difficult to suppress these carbonization reactions. It was reported that methylation of the phenolic -OH reduces the reactivity of phenolic intermediates and lowers the repolymerization rate when the reaction temperature is lower than 300 °C.[55] At higher reaction temperature (400 °C), methylated phenolics also become reactive and carbonization sets in. Based on these results, it is reasonable to argue that high reaction temperature is needed to effectively break down lignin, especially for technical lignin with its typical highly recalcitrant structure containing a large amount of C−C intralinkages. Alkylation, Guerbet, and esterification reactions are more effective in suppressing char formation in the moderate temperature range of 300−340 °C.

Figure 2 shows the elemental CHO analysis of the THF-soluble residue obtained after ethanolysis at different temperatures. Compared to the oxygen content of the parent lignin of 31%, the oxygen content decreased with increasing temperature to 10% after ethanolysis at 380 °C. The sharp decrease of the oxygen content is due to the substantial removal of oxygen-containing functional groups due to demethoxylation and hydrodeoxygenation reactions. This has been confirmed by GC-MS and 2D HSQC NMR analysis of the lignin oil and residue. Under optimized conditions, a monomers yield of 60 wt % was obtained after reaction at 380 °C for 8 h (entry 13 Table 1). The monomers distribution of this particular case has been discussed in our previous work.[54]

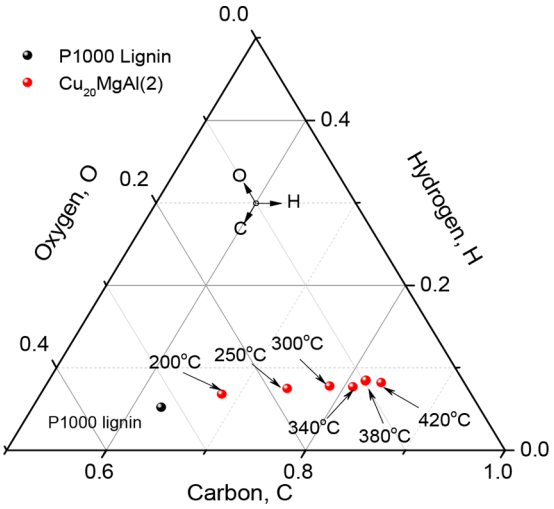


**Figure 2.** Elemental analysis of the parent lignin (black dot) and the THF-soluble lignin residue following reaction in ethanol at different temperatures for 4 h over the $Cu_{20}MgAl$ (2) mixed oxide catalyst (red dots).

**Ethanol Reactions with Lignin.** One of the important aspects of ethanolysis is the involvement of ethanol solvent in the lignin conversion reactions. Besides ethanol re-forming into hydrogen, ethanol also reacts with lignin by aromatic ring alkylation and Guerbet-type reactions with particular functional groups of lignin. Ethanol is also consumed by self-condensation reactions forming higher alcohols and esters via Guerbet-type reactions. Two typical lignin conversion reactions were carried out for this purpose, and the results are summarized in Table 3. Reaction at 340 °C for 4 h (30 wt % lignin monomers, entry 10 in Table 1) results in the recovery of about 71% of ethanol. The main reaction products derived from ethanol were $C_3$−$C_{11}$ alcohols and $C_4$−$C_{10}$ esters along with small amounts of aldehydes, ketones, and hydrocarbons. The total yield of these products was about 12 wt %. When the reaction was conducted at 380 °C for 8 h (60 wt % lignin monomers, entry 13 in Table 1), only 42% of ethanol could be recovered after the reaction. The finding that the amount of liquid reaction products was slightly lower indicates that ethanol re-forming was more extensive at the higher temperature.

We then employed carbon-14 ($^{14}C$) dating to estimate the amount of ethanol reacted with lignin by C-alkylation of aromatic rings and O-alkylation of the phenolic -OH groups and Guerbet-type reactions with other reactive groups of the lignin structure. The carbon-14 dating method can be used to distinguish carbon originating from biomass from carbon of fossil fuel origin. Biomass contains a certain fraction of $^{14}C$, close to the $^{14}C$ content of atmospheric $CO_2$. Fossil fuels, on the contrary, contain only very small amounts of $^{14}C$ due to its radioactive decay (half-life of 5730 years) over millions of years. Therefore, the fraction of $^{14}C$ can be used to estimate the fraction of biogenic carbon in an unknown sample. The application of $^{14}C$ measurements as tracer for biogenic and fossil carbon fractions has been demonstrated in several studies for a broad range of carbon-containing components.[57,58]

The principle of the method can, under specific conditions, also be used to investigate chemical processes.[59] In the present work, we used fossil-derived ethanol to study its introduction into biomass-derived lignin residue during ethanolysis. The $^{14}C$ contents of lignin and ethanol were determined as references. The absolute $^{14}C$ contents of ethanol and lignin were 0.48 ± 0.10 pMC and 105.40 ± 0.49 pMC, respectively. We analyzed samples originating from six reaction experiments in which the temperature was varied and determined the relative $^{14}C$ content expressed relative to the starting lignin for the THF-soluble and THF-insoluble residues and, for two reaction temperatures, also for char. The results of the carbon-14 dating analysis are shown in Table 4. We observe that the amount of ethanol-derived C atoms in the THF-soluble residue increases from 18% at 200 °C to 60% at 380 and 420 °C. The increasing inclusion of ethanol in the products is in qualitative agreement with the GC-MS and HSQC NMR results.[19,54] For the THF-insoluble lignin residue, the fraction of ethanol-derived C atoms is similar to that for the THF-soluble lignin residue at the same temperature, suggesting that capping reactions occur at similar rates for both fractions. We also analyzed the char originating from reactions at 380 and 420 °C and found that the inclusion of ethanol-derived C atoms was slightly lower than for the lignin residue samples. This can be explained by the lower reactivity


DOI: 10.1021/acssuschemeng.7b02790
ACS Sustainable Chem. Eng. 2017, 5, 10864−10874

**Table 3. Detailed Analysis the Mass Balances of Ethanol for Two Representative Lignin Conversion Reactions Using the $Cu_{20}MgAl(2)$ Catalyst**

| | | | | yield of ethanol conversion products (wt %) | | | | | | | |
|---|---|---|---|---|---|---|---|---|---|---|---|
| entry | temp (°C) | time (h) | ethanol recovery (wt %) | $C_3$–$C_{11}$ alcohols | $C_4$–$C_{10}$ esters | $C_2$–$C_4$ aldehydes | $C_4$–$C_7$ ethers | $C_3$–$C_9$ hydrocarbons | $C_4$–$C_7$ ketones | yield of $C_1$–$C_3$ gas products (wt %) | mass balance (wt %) |
| 1[a] | 340 | 4 | 70.5 | 7.3 | 2.5 | 1.0 | 0.3 | 0.7 | 0.0 | 1.4 | 83.7 |
| 2[b] | 380 | 8 | 42.0 | 6.9 | 2.1 | 1.2 | 0.4 | 2.3 | 0.7 | 5.3 | 60.9 |

[a]Entry 10 in Table 1. [b]Entry 13 in Table 1.

**Table 4. Carbon Fractions ($f_C$)[a] of Lignin and Ethanol in Lignin Residues Obtained from Reaction at Different Temperatures for 4 h over the CuMgAl Mixed Oxide Catalyst**

| | | | THF-soluble residue | | | | THF-insoluble residue | | | | char | | |
|---|---|---|---|---|---|---|---|---|---|---|---|---|---|
| | | | | $f_C$ (%) | | | | $f_C$ (%) | | | | $f_C$ (%) | |
| entry | temp (°C) | yield (wt %) | $^{14}$C value (pMC) | lignin | ethanol | yield (wt %) | $^{14}$C value (pMC) | lignin | ethanol | $^{14}$C value (pMC) | yield (wt %) | lignin | ethanol |
| 1 | 200 | 21 | 86.6 | 82 | 18 | 41 | 87.5 | 83 | 17 | | 1 | | |
| 2 | 250 | 35 | 64.3 | 61 | 39 | 59 | 67.5 | 64 | 36 | | 1 | | |
| 3 | 300 | 73 | 57.9 | 55 | 45 | 18 | 55.9 | 53 | 47 | | 0 | | |
| 4 | 340 | 69 | 55.4 | 53 | 47 | 9 | 51.0 | 48 | 52 | | 3 | | |
| 5 | 380[b] | 56 | 42.2 | 40 | 60 | 1 | | | | 55.2 | 6 | 52 | 48 |
| 6 | 420[b] | 55 | 41.5 | 39 | 61 | 0 | | | | 44.2 | 12 | 42 | 58 |

[a]Note: $f_C$ lignin means fraction of carbon from lignin. [b]Samples obtained from reactions using 100 mL autoclave.

**Table 5. Textual and Elemental Properties of Fresh and Regenerated $Cu_{20}MgAl(2)$ Catalysts**

| | | | | atomic ratios | | |
|---|---|---|---|---|---|---|
| catalyst | $S_{BET}$ ($m^2/g$) | $V^a$ ($cm^3/g$) | $D^b$ (nm) | Cu/Al | Mg/Al | (Cu + Mg)/Al |
| fresh | 189 | 0.53 | 15.6 | 0.48 | 1.73 | 2.20 |
| regenerated | 51 | 0.32 | 20.9 | 0.44 | 1.36 | 1.80 |

[a]Average pore volume. [b]Average pore diameter. [c]Element mass calculation is based on 0.5 g of fresh catalyst.

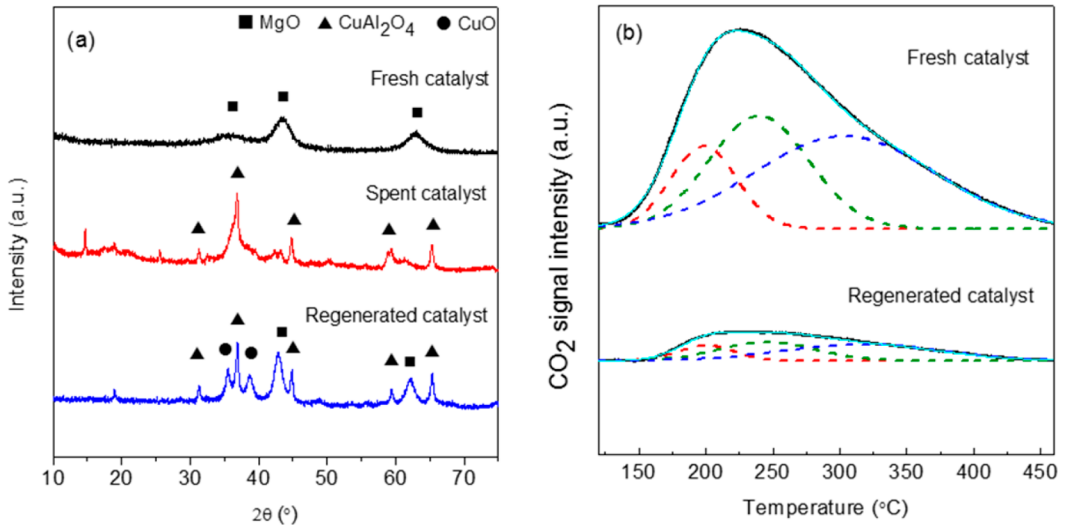


**Figure 3.** (a) XRD patterns of the fresh and regenerated $Cu_{20}MgAl(2)$ catalysts; (b) $CO_2$-TPD profiles of fresh, spent and regenerated $Cu_{20}MgAl(2)$ catalysts.

of the char fraction, implying that this byproduct became less reactive as reaction proceeds. These data confirm that the lignin monomers yield is strongly related to the capping reactions of reactive groups of lignin by ethanol.

**Catalyst Deactivation.** Catalyst deactivation is an important aspect in the realization of chemical processes at the industrial scale. We determined the reusability of the spent $Cu_{20}MgAl(2)$ catalyst employed at a temperature of 380 °C for 8 h, where the highest monomer yield was obtained (entry 13 in Table 1). Two reaction experiments were performed under similar conditions in order to obtain sufficient spent catalyst for characterization and recyclability evaluation. The solid residue which includes the catalyst was subjected to a regeneration procedure (calcination at 500 °C for 6 h) and then employed for another reaction. After this procedure, the performance of the recovered catalyst was significantly lower than that of the


DOI: 10.1021/acssuschemeng.7b02790
ACS Sustainable Chem. Eng. 2017, 5, 10864−10874

fresh one. It was also observed that the hot pressure was lower than in the experiment using the fresh catalyst. The lignin monomers yield decreased from 60 wt % (fresh catalyst) to 39 wt % (first recycle) and 16 wt % (second recycle). These changes demonstrate that the catalyst cannot be completely regenerated by calcination at 500 °C for 6 h. In order to gain insight into the cause of deactivation, XRD, ICP, and $CO_2$-TPD were used to characterize the fresh, spent, and regenerated catalyst samples.

The characterization results are summarized in Table 5 and Figure 3. The fresh $Cu_{20}MgAl(2)$ catalyst has a surface area of 189 $m^2/g$ and a pore volume of 0.53 $cm^3/g$. After reaction and regeneration, these values decreased to 51 $m^2/g$ and 0.32 $cm^3/g$. Elemental analysis shows that the Cu/Al ratio was slightly decreased from 0.48 in the fresh catalyst to 0.44 in the regenerated catalyst. The Mg/Al ratio decreased more pronouncedly from 1.73 to 1.36. XRD confirms that the amount of MgO decreased upon reaction and regeneration, suggesting together with elemental analysis that part of MgO has dissolved. XRD shows that a $CuAl_2O_4$ spinel oxide phase has formed. After regeneration of the spent catalyst, the spinel structure remains, while only part of the MgO phase is regenerated with a larger particle size as can be derived from the narrower diffraction peaks. Moreover, a CuO phase is present after regeneration indicating that the highly mixed nature of the Cu−Mg−Al components in the fresh catalyst is lost. We also determined the basic site density by $CO_2$-TPD. Compared to the fresh catalyst, the total basic site density was substantially lower in the regenerated catalyst. These findings indicate that deactivation of $Cu_{20}MgAl(2)$ is due to the leaching of the Mg. Regeneration by oxidation results in partial recovery of the MgO phase at the expense of its particle size. Importantly, a large part of the basic sites initially present in the original catalyst were lost, in part due to leaching of Mg and in part due to the lower surface area. We surmise that water produced during the reaction is a cause of Mg leaching from the mixed oxides.

**Depolymerization of Woody Biomass.** We also investigated the possibility to convert whole lignocellulosic biomass, i.e. softwood Scotch pine sawdust, at 300 and 340 °C. The reaction time was 4 h in both cases. GC-MS was used to analyze the product mixture. As in lignin conversion, we regarded cyclic monomer products as products from lignin. The analysis of the carbohydrate-derived products is challenging, as a wide range of long-chain aliphatic alcohols and esters were produced, some of them being similar to the ethanol conversion products. In order to estimate the amount of these products, a blank reaction without biomass was performed under similar conditions. The analysis of this mixture was used as a reference for distinguishing holocellulose (the total polysaccharide fraction of wood comprised of cellulose and hemicellulose) conversion products from ethanol conversion products. Only new peaks in the biomass conversion experiments were taken into account for product quantification. The yields of holocellulose monomers were estimated in this way and included in the product analysis reported in Table 6.

When the reaction was performed at 300 °C for 4 h using 1 g of wood sawdust, a yield of 19 wt % lignin products was obtained (Table 6, entry 1, based on a lignin content of 26.1 wt %). This yield is similar to the monomers yield obtained from the soda lignin under identical conditions (19 wt %). A yield of 36 wt % holocellulose conversion products was obtained (based on 58.2 wt % of the holocellulose content in SP wood). When we increased the wood loading to 3 g, a similar lignin monomers yield (20 wt %, Table 6, entry 2) was obtained. However, the yield of holocellulose conversion products decreased significantly. The total monomer yield (wood base) decreased from 26 to 12 wt %. Notably, by increasing the reaction temperature to 340 °C, the lignin monomers yield increased to 63 wt % at low biomass loading (lignin base, entry 3). The yield of holocellulose conversion products was also seen to increase. A total yield of 54 wt % (wood base) was obtained. Using 3 g of biomass led again to a lower lignin monomer yield. In any case, at 340 °C the lignin monomers yield obtained from Scotch pine biomass was substantially higher than the yield obtained from soda lignin under identical conditions (30 wt %, Table 1, entry 10). The total monomers yields of catalytic SP depolymerization at 340 °C for 1 and 3 g of SP were 54 and 29 wt %, respectively (Table 6, entries 3 and 4). Notably, the holocellulose conversion yield was more affected by the biomass loading than the lignin monomers yield. This suggests that it is easier to convert the native lignin in SP wood than the holocellulose fraction. Part of the recalcitrance of cellulose conversion is due to its crystalline nature. Table 7 shows the holocellulose conversion products obtained from reaction at 340 °C for 4 h using 1 g of SP wood as the feedstock. The main products were alcohols, aldehydes, alkanes, alkenes, esters, ethers, and ketones ranging in carbon number from 5 to 16. Ford and co-workers also reported the one-pot catalytic conversion of woody biomass into liquid fuels using a similar Cu-doped porous metal oxide in supercritical methanol at 300 °C and reported $C_2$−$C_6$ aliphatic alcohols as the main products.[16] In our case, longer chain products were formed, which is likely due to the involvement of ethanol in coupling reactions with holocellulose-derived short-chain aliphatic alcohols.

Figure 4 shows a representative lignin monomers distribution obtained from the SP wood feedstock after reaction at 340 °C for 4 h. The products were different from the ones obtained from the soda lignin. More oxygenated aromatics such as guaiacyl-type monomeric products were obtained from SP wood. This result indicates that the rate of deoxygenation is lower for woody biomass than for lignin. This could be due to the fact that native lignin in Scotch pine contains more oxygenated functional groups (e.g., -$OCH_3$ and -OH) than those in isolated P1000 lignin. Some of these functional groups are removed during the isolation process which results in less oxygen content. Besides, the competitive effects of the presence of sugars and products derived from the sugars might also play

**Table 6. Product Analysis of Catalytic Depolymerization of Scotch Pine Sawdust over the $Cu_{20}MgAl(2)$ Catalyst in Ethanol[a]**

| | | | lignin monomer yield (wt %) | | holocellulose monomer yield (wt %) | | sum of monomer yield (wt %) |
|---|---|---|---|---|---|---|---|
| entry | temp (°C) | SP loading (g) | lignin base | wood base | sugar base | wood base | wood base |
| 1 | 300 | 1.0 | 19 | 5 | 36 | 21 | 26 |
| 2 | 300 | 3.0 | 20 | 5 | 13 | 7 | 12 |
| 3 | 340 | 1.0 | 67 | 18 | 63 | 36 | 54 |
| 4 | 340 | 3.0 | 45 | 12 | 29 | 17 | 29 |

[a]Note: The lignin content of SP is 26.1 wt %, The holocellulose content is 58.2 wt %.



DOI: 10.1021/acssuschemeng.7b02790
ACS Sustainable Chem. Eng. 2017, 5, 10864−10874

Table 7. Yield of Cellulose and Hemicellulose Conversion Products of Depolymerization of Scotch Pine Sawdust at 340 °C for 4 h over the $Cu_{20}MgAl(2)$ Catalyst (Table 6, Entry 3)[a]

| name of compd | carbon no. | molecular yield(g/mol) | amount (mg) |
|---|---|---|---|
| alcohols | | | |
| 2-methyl-1-butanol | C5 | 88 | 34.0 |
| 3-hexen-1-ol | C6 | 100 | 10.3 |
| 1-hexen-3-ol | C6 | 100 | 3.5 |
| 2-hexen-1-ol | C6 | 100 | 11.6 |
| 5-methyl-1-heptanol | C8 | 130 | 19.5 |
| 2-propyl-1-heptanol | C10 | 158 | 34.1 |
| 2-decanol | C10 | 158 | 11.3 |
| 2-butyl-1-octanol | C12 | 186 | 7.2 |
| 2-hexyl-1-decanol | C16 | 242 | 5.1 |
| aldehydes | | | |
| 2-ethyl-2-butenal | C6 | 98 | 28.4 |
| octanal | C8 | 128 | 8.4 |
| 2-ethylhexanal | C8 | 128 | 2.9 |
| alkanes | | | |
| nonylcyclopropane | C12 | 168 | 4.8 |
| alkenes | | | |
| 3-methyl-2-heptene | C8 | 112 | 4.3 |
| 2-octene | C8 | 112 | 2.5 |
| 3-ethyl-3-hexene | C8 | 112 | 1.9 |
| 3-methyl-heptene | C8 | 112 | 1.2 |
| 6-methyl-1-heptene | C8 | 118 | 0.1 |
| 4-dodecene | C12 | 168 | 5.6 |
| esters | | | |
| 2-hydroxy-propanoic acid, ethyl ester | C5 | 118 | 8.5 |
| 3-methyl-butanoic acid, butyl ester | C9 | 158 | 6.9 |
| 2-methyl-propanoic acid, 2-methylbutyl ester | C9 | 158 | 2.5 |
| acetic acid, octyl ester | C10 | 172 | 4.8 |
| 2-ethyl-hexanoic acid, ethyl ester | C10 | 172 | 12.7 |
| 4-methyl-octanoic acid, ethyl ester | C11 | 186 | 10.1 |
| 2-ethyl butyl hexanoate | C12 | 200 | 19.4 |
| acetic acid, decyl ester | C12 | 200 | 9.9 |
| 4-ethyl butyl octanoate | C14 | 228 | 23.9 |
| 4-methyl octanoic acid, pentyl ester | C14 | 228 | 6.5 |
| dodecanoic acid, ethyl ester | C14 | 228 | 4.6 |
| octanoic acid, hexyl ester | C14 | 228 | 15.3 |
| ethers | | | |
| 1,1-diethoxybutane | C8 | 146 | 4.9 |
| ketones | | | |
| 2-methylcycloheptanone | C8 | 126 | 8.2 |
| 3-nonen-2-one | C9 | 140 | 15.8 |
| 3-decanone | C10 | 156 | 18.3 |
| internal standard (ISTD) | | | |
| *n*-dodecane | C12 | 170 | 7.5 |

[a]Note: The effective carbon number (ECN) method was applied to calculate the response factors of the compounds relative to the *n*-dodecane internal standard.[60]

a role in hindering deoxygenation.[47] We also evaluated the conversion of microcrystalline cellulose and glucose over the same catalyst in supercritical ethanol at 300 °C for 4 h, respectively. Catalytic depolymerization of cellulose led to a product yield of 52 wt %. In a similar experiment with glucose the product yield was 57 wt %. Mainly long-chain aliphatic alcohols and esters, similar to the compounds obtained from the carbohydrate fraction in SP wood, were obtained in these two experiments. These products are suitable for further fractionation or conversion to bulk chemicals, or can be directly used as fuel additives. These initial results demonstrate that woody biomass can be effectively converted into a wide range of aliphatic alcohols and esters in a single step. This avoids the costly pretreatment process of lignocellulosic biomass to separate lignin from the carbohydrate fraction.

## CONCLUSIONS

Biorefineries processing second-generation biomass require value to be added to all parts of the lignocellulosic biomass. We have demonstrated high-yield production of monomeric aromatics from lignin using a mixed oxide catalyst in supercritical ethanol with little char formation. The reaction temperature has a profound impact on the reaction outcome. Condensation reactions are dominant at low temperature


DOI: 10.1021/acssuschemeng.7b02790
ACS Sustainable Chem. Eng. 2017, 5, 10864−10874

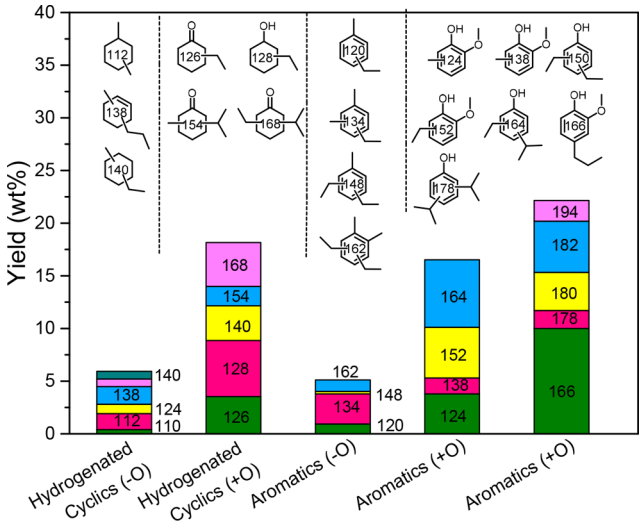


**Figure 4.** Lignin monomers distribution deriving from conversion of Scotch pine at 340 °C for 4 h over the $Cu_{20}MgAl(2)$ catalyst (Table 6, entry 3; the yield is based on 26.1 wt % lignin content in SP wood).

(200−250 °C), while char-forming reactions become significant at very high reaction temperature (380−420 °C). At low temperature, lignin depolymerization involves hydrogenolysis reactions; thermal cracking is nearly absent under these conditions, resulting in low monomers yield. As the rates of condensation reactions involving reactive side chains such as C═C double bonds and species such as formaldehyde are higher than that of hydrogenolysis, heavy residue is formed in this temperature regime. Moreover, the rates of reactions that can limit char formation such as alkylation, Guerbet, and esterification reactions are low below 300 °C. This shifts the balance toward condensation rather than depolymerization. At moderate temperature (300−340 °C), depolymerization reactions are enhanced, mostly because thermal cracking starts, and the more recalcitrant bonds in typical lignins can be cleaved including those of heavy residue formed during heating. This generates more lignin fragments and reactive phenolic intermediates. The reactive phenolic intermediates are obtained in higher proportion, because they are protected by alkylation, Guerbet, and esterification reactions. This promotes depolymerization. At the highest temperatures used in this study (380−420 °C), char-forming reactions due to carbonization become dominant. These carbonization reactions cannot be suppressed. However, higher reaction temperature results in a significant loss of ethanol solvent due to conversion. The radiocarbon (carbon-14) dating analysis of the lignin residue revealed that about half of the carbon in the lignin residue originated from ethanol after reaction at 380 °C for 8 h. A recyclability test of the spent catalyst showed significant decrease in catalytic activity. The loss of basic sites due to hydrolysis of MgO and a concomitant loss of surface area due to spinel oxide formation of the Cu and Al components were identified as the main causes of the lower activity of regenerated catalysts. The utility of this process to upgrade directly woody biomass (Scotch pine) was explored at 300 and 340 °C for 4 h. A wide range of products including alcohols, aldehydes, alkanes, alkenes, esters, ethers, and ketones with 5−14 carbon atoms was obtained by conversion of holocellulose. The monomer yield was 63 wt % based on holocellulose. The major products are aliphatic alcohols and esters. Conversion of the lignin contained in the woody biomass is more facile than conversion of technical lignin. Up to 67 wt % monomer yield (lignin base) could be obtained. The overall yield of aromatic and long-chain aliphatic products is 54 wt % (wood base).

## EXPERIMENTAL SECTION

**Chemicals and Materials.** Protobind 1000 alkali lignin was purchased from GreenValue. It was produced by soda pulping of wheat straw (sulfur-free lignin with less than 4 wt % carbohydrates and less than 2 wt % ash). Scotch pine (SP, also known as Scots pine) was harvested from a field in the vicinity of Bursa, Turkey in 2014 and chopped into small pieces on site. SP was used in the form of sawdust in the reaction experiments. First, a suitable amount of SP was milled and sieved to a particle size below 125 $\mu$m and then dried at 105 °C for 12 h before use. The detailed composition of SP can be found in Table 8. Microcrystalline cellulose and D-(+)-glucose were purchased from Sigma-Aldrich. All commercial chemicals were analytical reagents and were used without further purification.

**Catalyst Preparation.** A 20 wt % Cu-containing MgAl mixed oxide ($CuMgAlO_x$) catalyst was prepared by a coprecipitation method with a fixed $M^{2+}/M^{3+}$ atomic ratio of 2. $CuMgAlO_x$ (6 g) was prepared in the following way: 4.40 g of $Cu(NO_3)_2{\cdot}2.5\ H_2O$, 15.67 g of $Mg(NO_3)_2{\cdot}6H_2O$, and 15.01 g of $Al(NO_3)_3{\cdot}9\ H_2O$ were dissolved in 100 mL of deionized water. This solution and 100 mL of a NaOH (9.60 g) solution were slowly added (1 drop/s) through 100 mL dropping funnels to 250 mL of $Na_2CO_3$ (5.09 g) solution in a 1000 mL necked flask at 60 °C under vigorous stirring, while keeping the pH of the slurry at 10. When addition was complete after 45 min, the milk-like light-blue slurry was aged at 60 °C under stirring for 24 h. The precipitate was filtered and washed with distilled water until the filtrate reached a pH of 7. The solid was dried overnight at 105 °C and ground and sieved to a particle size below 125 $\mu$m. The hydrotalcite structure of the obtained powder was confirmed by XRD. This precursor was calcined at a heating rate of 2 °C/min from 40 to 460 °C and kept at this temperature for 6 h in static air. The resulting catalyst was denoted by $Cu_{20}MgAl(2)$.

**Catalytic Activity Measurements.** AmAr stirred high-pressure 50 mL autoclaves were used to study the (catalytic) conversion of lignin in (m)ethanol. Typically, the autoclave was charged with a suspension of 500 mg of catalyst and 1000 mg of lignin in 20 mL of solvent. An amount of 10 $\mu$L of *n*-dodecane was added as the internal standard. The reactor was sealed and purged with nitrogen several times to remove oxygen. After leak testing, the pressure was set to 10 bar and the reaction mixture was heated to the desired reaction temperature under continuous stirring at 500 rpm within 1 h. After the reaction, the heating oven was removed and the reactor was allowed to cool to room temperature. For those reactions conducted at 100 mL Parr autoclaves, the same procedure was applied. The only difference is that 40 mL of solvent was applied and the same amount of *n*-dodecane internal standard was added after reaction. A workup procedure was developed to distinguish light (THF-soluble) lignin fragments and heavy (THF-insoluble) lignin fragments (THF = tetrahydrofuran) and char. A detailed description of this workup procedure can be found in our previous report.[47]

**Table 8. Detailed Composition Analysis Results of the Scotch Pine**[a]

| sample name | total sugars | glucose | xylose | mannose | arabinose | galactose | rhamnose | Klason lignin | acid-soluble lignin | extractives | ash |
|---|---|---|---|---|---|---|---|---|---|---|---|
| Scotch pine | 58.22 | 39.75 | 5.24 | 10.17 | 1.19 | 1.73 | 0.12 | 25.70 | 0.45 | 9.47 | 0.35 |

[a]Note: All data are presented as weight percent of total dry matter. Detailed analysis approach can be referred to in ref 47.



DOI: 10.1021/acssuschemeng.7b02790
ACS Sustainable Chem. Eng. 2017, 5, 10864−10874

**Lignin Product Analysis.** The liquid phase product mixture were analyzed by a Shimadzu 2010 GC-MS system equipped with a RTX-1701 column (60 m × 0.25 mm × 0.25 μm) and a flame ionization detector (FID) together with a mass spectrometer detector. Identification of products was achieved based on a search of the MS spectra with the NIST11 and NIST11s MS libraries. The peaks with the same molecular weight ($M_w$) were unified and presented by the structure determined by (1D) GC-MS and/or (2D) GC × GC-MS (details can be found in our previous work[19]). These products were further divided into four groups, namely, hydrogenated cyclics (−o (oxygen-free)), hydrogenated cyclics (+o (oxygen-containing)), aromatics (−o), and aromatics (+o), according to the nature of the ring structure and functional groups. All the quantitative analyses of liquid phase product were based on 1D GC-FID. Experimentally determined weight response factors of cyclohexane, cyclohexanone, ethyl benzene, and ethyl guaiacol were used for these four groups related to *n*-dodecane as the internal standard. The yields of lignin residue, monomers and char were calculated by using eqs 1−4.

$$\text{yield of monomers/(wt \%)} = \frac{\text{wt of monomers (calcd from GC-FID)}}{\text{wt of starting Protobind lignin}} \times 100 \quad (1)$$

$$\text{yield of THF-soluble residue/(wt \%)} = \frac{\text{wt of THF-soluble residue}}{\text{wt of starting Protobind lignin}} \times 100 \quad (2)$$

$$\text{yield of THF-insoluble residue/(wt \%)} = \frac{\text{wt of THF-insoluble residue}}{\text{wt of starting Protobind lignin}} \times 100 \quad (3)$$

$$\text{yield of char/(wt \%)} = \frac{\text{wt of char and undissolved catalyst} \times \text{wt loss in TGA}}{\text{wt of starting Protobind lignin}} \times 100 \quad (4)$$

**Gel Permeation Chromatography.** GPC analyses were performed by using a Shimadzu Prominence-I LC-2030C 3D apparatus equipped with two columns connected in series (mixed-C and mixed-D, Polymer Laboratories) and a UV−vis detector at 254 nm. The column was calibrated with polystyrene standards. Analyses were carried out at 25 °C using THF as eluent with a flow rate of 1 mL/min. For the lignin residue analysis, the sample was prepared at a concentration of 2 mg/mL. All the samples were filtered using a 0.45 μm filter membrane prior to injection.

**Elemental Analysis (CHO).** The carbon, hydrogen, and oxygen (CHO) contents of the lignin residue were quantitatively determined by means of elemental analysis (PerkinElmer 2400 series II Elemental Analyzer, CHN mode). The lignin samples were dried overnight in a vacuum oven at 60 °C to remove residual water and solvent. Carbon and hydrogen analysis was conducted by combustion followed by thermal conductivity and infrared detection of effluent gases. The oxygen content was determined by considering that the material consisted of C, O, and H atoms.

**Elemental Analysis (ICP).** The metal contents of the fresh and spent catalysts were determined by inductively coupled plasma atomic emission spectrometry (ICP-AES) on a Spectro Ciros CCD ICP optical emission spectrometer with axial plasma viewing. All the samples were dissolved in an equivolumetric mixture of $H_2O$ and $H_2SO_4$.

**X-ray Powder Diffraction.** Powder X-ray diffraction (XRD) was measured on a Bruker Endeavor D4 with Cu Kα radiation (40 kV and 30 mA). They were recorded with 0.02° steps over the 5−80° angular range with 0.2 s counting time per step.

**Temperature Programmed Desorption of $CO_2$.** Temperature programmed desorption of $CO_2$ ($CO_2$-TPD) was carried out in a home-built reactor system coupled to a mass spectrometer. After pretreatment at 460 °C for 1 h in a flow of 50 mL/min He, the sample (50 mg) was cooled to 100 °C and exposed to $CO_2$ (25 vol % in He) for 0.5 h. After sweeping with He for 1 h to remove physisorbed $CO_2$, the temperature was increased linearly at a rate of 10 °C/min in He and the signal of $CO_2$ ($m/e$ = 44) was recorded by online mass spectrometry (quadrupole mass spectrometer, Balzers Omnistar). The amount of $CO_2$ was quantified by a calibration curve, which was established by thermal decomposition of known amounts of $NaHCO_3$.

**Carbon-14 dating.** A small aliquot of each sample material was weighted in a small tin capsule and combusted to $CO_2$ in an elemental analyzer (combined Elementar Isotope Cube-Isoprime 100 system). To obtain approximately 4 mL of $CO_2$ (2 mg of C), the size of each sample was based on its estimated carbon content determined by elemental analysis. For the lignin and lignin residue samples the weights of the samples were between 2.47 and 3.23 mg, and for the catalyst/char samples the weights were 11.22 and 15.46 mg. A small part of the $CO_2$ was let into an isotope ratio mass spectrometer (IRMS) to measure the $^{13}C$ content (measured relative to a reference material). The rest of the $CO_2$ was cryogenically (liquid $N_2$, −196 °C) trapped in a flask and remaining gases (such as the helium carrier gas) were pumped away. The $CO_2$ was then graphitized to pure solid C at a certain temperature, with $H_2$ and using a Fe powder as catalyst. The graphite was pressed in a target and then measured for carbon isotope abundances of $^{12}C$, $^{13}C$, and $^{14}C$ with a $^{14}C$-dedicated accelerator mass spectrometer (AMS). The amount of carbon-14 is calculated by convention relative to measured standardized reference materials and standardized reference values, including correction for background counts and isotope fractionation. (See the literature for more detailed information on the calculations.[61]) The amounts of carbon-14 in biobased or fossil carbon materials are usually expressed as pMC (i.e., the percentage relative to the measured and standardized reference material).

The fractions of lignin-based and ethanol-based carbon ($f_{C_{lignin}}$ and $f_{C_{ethanol}}$, respectively) in the different sample materials were calculated as follows based on the measured $^{14}C$ values in the separate lignin and ethanol and the sample itself (as $^{14}C_{sample} = {}^{14}C_{lignin} f_{C_{lignin}} + {}^{14}C_{ethanol} f_{C_{ethanol}}$):

$$f_{C_{lignin}} = ({}^{14}C_{sample} - {}^{14}C_{ethanol})/({}^{14}C_{lignin} - {}^{14}C_{ethanol})$$

$$f_{C_{ethanol}} = 1 - f_{C_{lignin}}$$

## AUTHOR INFORMATION


### Corresponding Author

*E-mail: e.j.m.hensen@tue.nl.

### ORCID

Emiel J. M. Hensen: 0000-0002-9754-2417


### Notes

The authors declare no competing financial interest.

## ACKNOWLEDGMENTS

This work was performed under the framework of Chemelot InSciTe and is supported by contributions from the European Interreg V Flanders, the European Regional Development Fund (ERDF), the province of Brabant and Limburg, and the Dutch Ministry of Economy.

## REFERENCES

(1) Zakzeski, J.; Bruijnincx, P. C. A.; Jongerius, A. L.; Weckhuysen, B. M. The Catalytic Valorization of Lignin for the Production of Renewable Chemicals. *Chem. Rev.* **2010**, *110*, 3552−3599.

(2) Xu, W. Y.; Miller, S. J.; Agrawal, P. K.; Jones, C. W. Depolymerization and Hydrodeoxygenation of Switchgrass Lignin with Formic Acid. *ChemSusChem* **2012**, *5*, 667−675.



DOI: 10.1021/acssuschemeng.7b02790
*ACS Sustainable Chem. Eng.* 2017, 5, 10864−10874

(3) Deuss, P. J.; Barta, K. From models to lignin: Transition metal catalysis for selective bond cleavage reactions. *Coord. Chem. Rev.* **2016**, *306*, 510−532.
(4) Ragauskas, A. J.; Beckham, G. T.; Biddy, M. J.; Chandra, R.; Chen, F.; Davis, M. F.; Davison, B. H.; Dixon, R. A.; Gilna, P.; Keller, M.; Langan, P.; Naskar, A. K.; Saddler, J. N.; Tschaplinski, T. J.; Tuskan, G. A.; Wyman, C. E. Lignin valorization: improving lignin processing in the biorefinery. *Science* **2014**, *344*, 1246843.
(5) Holladay, J. E.; White, J. F.; Bozell, J. J.; Johnson, D. *Top Value-Added Chemicals from Biomass - Vol. II—Results of Screening for Potential Candidates from Biorefinery Lignin*, PNNL-16983; Pacific Northwest National Laboratory (PNNL): Richland, WA, USA, 2007; http://www.pnl.gov/main/publications/external/technical_reports/PNNL-16983.pdf.
(6) Azadi, P.; Inderwildi, O. R.; Farnood, R.; King, D. A. Liquid fuels, hydrogen and chemicals from lignin: A critical review. *Renewable Sustainable Energy Rev.* **2013**, *21*, 506−523.
(7) Li, C. Z.; Zhao, X. C.; Wang, A. Q.; Huber, G. W.; Zhang, T. Catalytic Transformation of Lignin for the Production of Chemicals and Fuels. *Chem. Rev.* **2015**, *115*, 11559−11624.
(8) Joffres, B.; Laurenti, D.; Charon, N.; Daudin, A.; Quignard, A.; Geantet, C. Thermochemical Conversion of Lignin for Fuels and Chemicals: A Review. *Oil Gas Sci. Technol.* **2013**, *68*, 753−763.
(9) Pandey, M. P.; Kim, C. S. Lignin Depolymerization and Conversion: A Review of Thermochemical Methods. *Chem. Eng. Technol.* **2011**, *34*, 29−41.
(10) Rinaldi, R.; Jastrzebski, R.; Clough, M. T.; Ralph, J.; Kennema, M.; Bruijnincx, P. C.; Weckhuysen, B. M. Paving the Way for Lignin Valorisation: Recent Advances in Bioengineering, Biorefining and Catalysis. *Angew. Chem., Int. Ed.* **2016**, *55*, 8164−215.
(11) Miller, J. E.; Evans, L.; Littlewolf, A.; Trudell, D. E. Batch microreactor studies of lignin and lignin model compound depolymerization by bases in alcohol solvents. *Fuel* **1999**, *78*, 1363−1366.
(12) Roberts, V. M.; Stein, V.; Reiner, T.; Lemonidou, A.; Li, X. B.; Lercher, J. A. Towards Quantitative Catalytic Lignin Depolymerization. *Chem. - Eur. J.* **2011**, *17*, 5939−5948.
(13) Onwudili, J. A.; Williams, P. T. Catalytic depolymerization of alkali lignin in subcritical water: influence of formic acid and Pd/C catalyst on the yields of liquid monomeric aromatic products. *Green Chem.* **2014**, *16*, 4740−4748.
(14) Zhang, J. G.; Teo, J.; Chen, X.; Asakura, H.; Tanaka, T.; Teramura, K.; Yan, N. A Series of NiM (M = Ru, Rh, and Pd) Bimetallic Catalysts for Effective Lignin Hydrogenolysis in Water. *ACS Catal.* **2014**, *4*, 1574−1583.
(15) Barta, K.; Matson, T. D.; Fettig, M. L.; Scott, S. L.; Iretskii, A. V.; Ford, P. C. Catalytic disassembly of an organosolv lignin via hydrogen transfer from supercritical methanol. *Green Chem.* **2010**, *12*, 1640−1647.
(16) Matson, T. D.; Barta, K.; Iretskii, A. V.; Ford, P. C. One-Pot Catalytic Conversion of Cellulose and of Woody Biomass Solids to Liquid Fuels. *J. Am. Chem. Soc.* **2011**, *133*, 14090−14097.
(17) Song, Q.; Wang, F.; Cai, J. Y.; Wang, Y. H.; Zhang, J. J.; Yu, W. Q.; Xu, J. Lignin depolymerization (LDP) in alcohol over nickel-based catalysts via a fragmentation-hydrogenolysis process. *Energy Environ. Sci.* **2013**, *6*, 994−1007.
(18) Zhang, X. H.; Zhang, Q.; Wang, T. J.; Ma, L. L.; Yu, Y. X.; Chen, L. G. Hydrodeoxygenation of lignin-derived phenolic compounds to hydrocarbons over Ni/$SiO_2$-$ZrO_2$ catalysts. *Bioresour. Technol.* **2013**, *134*, 73−80.
(19) Huang, X.; Korányi, T. I.; Boot, M. D.; Hensen, E. J. M. Catalytic Depolymerization of Lignin in Supercritical Ethanol. *ChemSusChem* **2014**, *7*, 2276−2288.
(20) Ma, R.; Hao, W. Y.; Ma, X. L.; Tian, Y.; Li, Y. D. Catalytic Ethanolysis of Kraft Lignin into High-Value Small-Molecular Chemicals over a Nanostructured alpha-Molybdenum Carbide Catalyst. *Angew. Chem., Int. Ed.* **2014**, *53*, 7310−7315.
(21) Zhang, X.; Zhang, Q.; Long, J.; Xu, Y.; Wang, T.; Ma, L.; Li, Y. Phenolics Production through Catalytic Depolymerization of Alkali Lignin with Metal Chlorides. *BioResources* **2014**, *9*, 3347−3360.
(22) Zhang, X.; Zhang, Q.; Wang, T.; Li, B.; Xu, Y.; Ma, L. Efficient upgrading process for production of low quality fuel from bio-oil. *Fuel* **2016**, *179*, 312−321.
(23) Wang, X. Y.; Rinaldi, R. Solvent Effects on the Hydrogenolysis of Diphenyl Ether with Raney Nickel and their Implications for the Conversion of Lignin. *ChemSusChem* **2012**, *5*, 1455−1466.
(24) Zakzeski, J.; Weckhuysen, B. M. Lignin Solubilization and Aqueous Phase Reforming for the Production of Aromatic Chemicals and Hydrogen. *ChemSusChem* **2011**, *4*, 369−378.
(25) Jongerius, A. L.; Bruijnincx, P. C. A.; Weckhuysen, B. M. Liquid-phase reforming and hydrodeoxygenation as a two-step route to aromatics from lignin. *Green Chem.* **2013**, *15*, 3049−3056.
(26) Cheng, S. N.; Wilks, C.; Yuan, Z. S.; Leitch, M.; Xu, C. B. Hydrothermal degradation of alkali lignin to bio-phenolic compounds in sub/supercritical ethanol and water-ethanol co-solvent. *Polym. Degrad. Stab.* **2012**, *97*, 839−848.
(27) Guvenatam, B.; Heeres, E. H. J.; Pidko, E. A.; Hensen, E. J. M. Lewis acid-catalyzed depolymerization of soda lignin in supercritical ethanol/water mixtures. *Catal. Today* **2016**, *269*, 9−20.
(28) Deuss, P. J.; Scott, M.; Tran, F.; Westwood, N. J.; de Vries, J. G.; Barta, K. Aromatic Monomers by in Situ Conversion of Reactive Intermediates in the Acid-Catalyzed Depolymerization of Lignin. *J. Am. Chem. Soc.* **2015**, *137*, 7456−7467.
(29) Deuss, P. J.; Lahive, C. W.; Lancefield, C. S.; Westwood, N. J.; Kamer, P. C. J.; Barta, K.; de Vries, J. G. Metal Triflates for the Production of Aromatics from Lignin. *ChemSusChem* **2016**, *9*, 2974−2981.
(30) Deepa, A. K.; Dhepe, P. L. Lignin Depolymerization into Aromatic Monomers over Solid Acid Catalysts. *ACS Catal.* **2015**, *5*, 365−379.
(31) Oregui-Bengoechea, M.; Gandarias, I.; Arias, P. L.; Barth, T. Unraveling the Role of Formic Acid and the Type of Solvent in the Catalytic Conversion of Lignin: A Holistic Approach. *ChemSusChem* **2017**, *10*, 754−766.
(32) Jastrzebski, R.; Constant, S.; Lancefield, C. S.; Westwood, N. J.; Weckhuysen, B. M.; Bruijnincx, P. C. Tandem Catalytic Depolymerization of Lignin by Water-Tolerant Lewis Acids and Rhodium Complexes. *ChemSusChem* **2016**, *9*, 2074−9.
(33) Wang, X. Y.; Rinaldi, R. Exploiting H-transfer reactions with RANEY (R) Ni for upgrade of phenolic and aromatic biorefinery feeds under unusual, low-severity conditions. *Energy Environ. Sci.* **2012**, *5*, 8244−8260.
(34) Wang, X. Y.; Rinaldi, R. A Route for Lignin and Bio-Oil Conversion: Dehydroxylation of Phenols into Arenes by Catalytic Tandem Reactions. *Angew. Chem., Int. Ed.* **2013**, *52*, 11499−11503.
(35) Zhang, J. G.; Asakura, H.; van Rijn, J.; Yang, J.; Duchesne, P.; Zhang, B.; Chen, X.; Zhang, P.; Saeys, M.; Yan, N. Highly efficient, NiAu-catalyzed hydrogenolysis of lignin into phenolic chemicals. *Green Chem.* **2014**, *16*, 2432−2437.
(36) Ma, X.; Ma, R.; Hao, W.; Chen, M.; Yan, F.; Cui, K.; Tian, Y.; Li, Y. Common Pathways in Ethanolysis of Kraft Lignin to Platform Chemicals over Molybdenum-Based Catalysts. *ACS Catal.* **2015**, *5*, 4803−4813.
(37) Zhang, X. H.; Wang, T. J.; Ma, L. L.; Zhang, Q.; Huang, X. M.; Yu, Y. X. Production of cyclohexane from lignin degradation compounds over Ni/$ZrO_2$-$SiO_2$ catalysts. *Appl. Energy* **2013**, *112*, 533−538.
(38) Sturgeon, M. R.; O'Brien, M. H.; Ciesielski, P. N.; Katahira, R.; Kruger, J. S.; Chmely, S. C.; Hamlin, J.; Lawrence, K.; Hunsinger, G. B.; Foust, T. D.; Baldwin, R. M.; Biddy, M. J.; Beckham, G. T. Lignin depolymerisation by nickel supported layered-double hydroxide catalysts. *Green Chem.* **2014**, *16*, 824−835.
(39) Singh, S. K.; Ekhe, J. D. Cu-Mo doped zeolite ZSM-5 catalyzed conversion of lignin to alkyl phenols with high selectivity. *Catal. Sci. Technol.* **2015**, *5*, 2117−2124.


DOI: 10.1021/acssuschemeng.7b02790
*ACS Sustainable Chem. Eng.* 2017, 5, 10864−10874

(40) Molinari, V.; Clavel, G.; Graglia, M.; Antonietti, M.; Esposito, D. Mild Continuous Hydrogenolysis of Kraft Lignin over Titanium Nitride-Nickel Catalyst. *ACS Catal.* **2016**, *6*, 1663−1670.
(41) Kumar, C. R.; Anand, N.; Kloekhorst, A.; Cannilla, C.; Bonura, G.; Frusteri, F.; Barta, K.; Heeres, H. J. Solvent free depolymerization of Kraft lignin to alkyl-phenolics using supported NiMo and CoMo catalysts. *Green Chem.* **2015**, *17*, 4921−4930.
(42) Long, J. X.; Xu, Y.; Wang, T. J.; Yuan, Z. Q.; Shu, R. Y.; Zhang, Q.; Ma, L. Efficient base-catalyzed decomposition and in situ hydrogenolysis process for lignin depolymerization and char elimination. *Appl. Energy* **2015**, *141*, 70−79.
(43) Singh, S. K.; Ekhe, J. D. Towards effective lignin conversion: HZSM-5 catalyzed one-pot solvolytic depolymerization/hydrodeoxygenation of lignin into value added compounds. *RSC Adv.* **2014**, *4*, 27971−27978.
(44) Parsell, T.; Yohe, S.; Degenstein, J.; Jarrell, T.; Klein, I.; Gencer, E.; Hewetson, B.; Hurt, M.; Kim, J. I.; Choudhari, H.; Saha, B.; Meilan, R.; Mosier, N.; Ribeiro, F.; Delgass, W. N.; Chapple, C.; Kenttamaa, H. I.; Agrawal, R.; Abu-Omar, M. M. A synergistic biorefinery based on catalytic conversion of lignin prior to cellulose starting from lignocellulosic biomass. *Green Chem.* **2015**, *17*, 1492−1499.
(45) Renders, T.; Schutyser, W.; Van den Bosch, S.; Koelewijn, S. F.; Vangeel, T.; Courtin, C. M.; Sels, B. F. Influence of Acidic ($H_3PO_4$) and Alkaline (NaOH) Additives on the Catalytic Reductive Fractionation of Lignocellulose. *ACS Catal.* **2016**, *6*, 2055−2066.
(46) Schutyser, W.; Van den Bosch, S.; Renders, T.; De Boe, T.; Koelewijn, S. F.; Dewaele, A.; Ennaert, T.; Verkinderen, O.; Goderis, B.; Courtin, C. M.; Sels, B. F. Influence of bio-based solvents on the catalytic reductive fractionation of birch wood. *Green Chem.* **2015**, *17*, 5035−5045.
(47) Huang, X.; Zhu, J.; Koranyi, T. I.; Boot, M. D.; Hensen, E. J. Effective Release of Lignin Fragments from Lignocellulose by Lewis Acid Metal Triflates in the Lignin-First Approach. *ChemSusChem* **2016**, *9*, 3262−3267.
(48) Huang, X.; Morales Gonzalez, O. M.; Zhu, J.; Korányi, T. I.; Boot, M. D.; Hensen, E. J. M. Reductive fractionation of woody biomass into lignin monomers and cellulose by tandem metal triflate and Pd/C catalysis. *Green Chem.* **2017**, *19*, 175−187.
(49) Galkin, M. V.; Smit, A. T.; Subbotina, E.; Artemenko, K. A.; Bergquist, J.; Huijgen, W. J.; Samec, J. S. Hydrogen-free catalytic fractionation of woody biomass. *ChemSusChem* **2016**, *9*, 3280−3287.
(50) Anderson, E. M.; Katahira, R.; Reed, M.; Resch, M. G.; Karp, E. M.; Beckham, G. T.; Román-Leshkov, Y. Reductive Catalytic Fractionation of Corn Stover Lignin. *ACS Sustainable Chem. Eng.* **2016**, *4*, 6940−6950.
(51) Li, C. Z.; Zheng, M. Y.; Wang, A. Q.; Zhang, T. One-pot catalytic hydrocracking of raw woody biomass into chemicals over supported carbide catalysts: simultaneous conversion of cellulose, hemicellulose and lignin. *Energy Environ. Sci.* **2012**, *5*, 6383−6390.
(52) Barta, K.; Ford, P. C. Catalytic Conversion of Nonfood Woody Biomass Solids to Organic Liquids. *Acc. Chem. Res.* **2014**, *47*, 1503−1512.
(53) Huang, X.; Atay, C.; Korányi, T. I.; Boot, M. D.; Hensen, E. J. M. Role of Cu−Mg−Al Mixed Oxide Catalysts in Lignin Depolymerization in Supercritical Ethanol. *ACS Catal.* **2015**, *5*, 7359−7370.
(54) Huang, X.; Korányi, T. I.; Boot, M. D.; Hensen, E. J. M. Ethanol as capping agent and formaldehyde scavenger for efficient depolymerization of lignin to aromatics. *Green Chem.* **2015**, *17*, 4941−4950.
(55) Nakamura, T.; Kawamoto, H.; Saka, S. Pyrolysis behavior of Japanese cedar wood lignin studied with various model dimers. *J. Anal. Appl. Pyrolysis* **2008**, *81*, 173−182.
(56) Constant, S.; Wienk, H. L. J.; Frissen, A. E.; de Peinder, P.; Boelens, R.; van Es, D. S.; Grisel, R. J. H.; Weckhuysen, B. M.; Huijgen, W. J. J.; Gosselink, R. J. A.; Bruijnincx, P. C. A. New insights into the structure and composition of technical lignins: a comparative characterisation study. *Green Chem.* **2016**, *18*, 2651−2665.
(57) Clayton, G. D.; Arnold, J. R.; Patty, F. A. Determination of Sources of Particulate Atmospheric Carbon. *Science* **1955**, *122*, 751−753.
(58) Currie, L. A.; Klouda, G. A.; Klinedinst, D. B.; Sheffield, A. E.; Jull, A. J. T.; Donahue, D. J.; Connolly, M. V. Fossil-Mass and Bio-Mass Combustion - C-14 for Source Identification, Chemical Tracer Development, and Model Validation. *Nucl. Instrum. Methods Phys. Res., Sect. B* **1994**, *92*, 404−409.
(59) Palstra, S. W. L.; Rabou, L. P. L. M.; Meijer, H. A. J. Radiocarbon-based determination of biogenic and fossil carbon partitioning in the production of synthetic natural gas. *Fuel* **2015**, *157*, 177−182.
(60) Grob, R. L.; Barry, E. F. *Modern Practice of Gas Chromatography*, 4th ed.; John Wiley & Sons: Hoboken, NJ, USA, 2004; DOI: 10.1002/0471651141.
(61) Palstra, S. W. L. On 14C-based methods for measuring the biogenic carbon fraction in fuels and flue gases. Ph.D. Dissertation, University of Groningen, Groningen, The Netherlands, 2016.


DOI: 10.1021/acssuschemeng.7b02790
*ACS Sustainable Chem. Eng.* 2017, 5, 10864−10874